

# Heightmap Reconstruction of Macula on Color Fundus Images Using Conditional Generative Adversarial Networks

Peyman Tahghighi\*, Reza A.Zoroofi\*, Sare Safi †, and Alireza Ramezani‡ §

\*School of Electrical and Computer Engineering  
University of Tehran, Tehran, Iran

†Ophthalmic Research Center, Research Institute for Ophthalmology and Vision Science  
Shahid Beheshti University of Medical Sciences, Tehran, Iran

‡Ophthalmic Epidemiology Research Center, Research Institute for Ophthalmology and Vision Science  
Shahid Beheshti University of Medical Sciences, Tehran, Iran

§Negah Specialty Ophthalmic Research Center  
Shahid Beheshti University of Medical Sciences, Tehran, Iran  
Email: peyman.tahghighi@ut.ac.ir

**Abstract**—For screening, 3D shape of the eye retina often provides structural information and can assist ophthalmologists to diagnose diseases. However, fundus images which are one of the most common screening modalities for retina diagnosis lack this information due to their 2D nature. Hence, in this work, we try to infer about this 3D information or more specifically its heights. Recent approaches have used shading information for reconstructing the heights but their output is not accurate since the utilized information is not sufficient. Additionally, other methods were dependent on the availability of more than one image of the eye which is not available in practice. In this paper, motivated by the success of Conditional Generative Adversarial Networks (cGANs) and deeply supervised networks, we propose a novel architecture for the generator which enhances the details in a sequence of steps. Comparisons on our dataset illustrate that the proposed method outperforms all of the state-of-the-art methods in image translation and medical image translation on this particular task. Additionally, clinical studies also indicate that the proposed method can provide additional information for ophthalmologists for diagnosis.

**Index Terms**—Conditional generative adversarial networks, Convolutional neural networks, Fundus image, Deep learning

## I. INTRODUCTION

A major and ubiquitous imaging technique for the eye is the fundus camera. However, due to its 2D nature, it lacks a considerable amount of data such as information about elevations in different parts and also the different number of views. Optical Coherence Tomography (OCT) [1] is an expensive but vital tool for retinal structure diagnosis which provides ophthalmologists with valuable information, enabling them to diagnose most of the retinal diseases such as glaucoma, diabetic and macular degeneration[2]. Nevertheless, owing to the cost of using this system, it is not common and using fundus images is mostly common for screening.

Shape from shading (SFS) [3] is the only method applied to this problem for the reconstruction of the height of a single fundus image [4]. However, the result generated by this

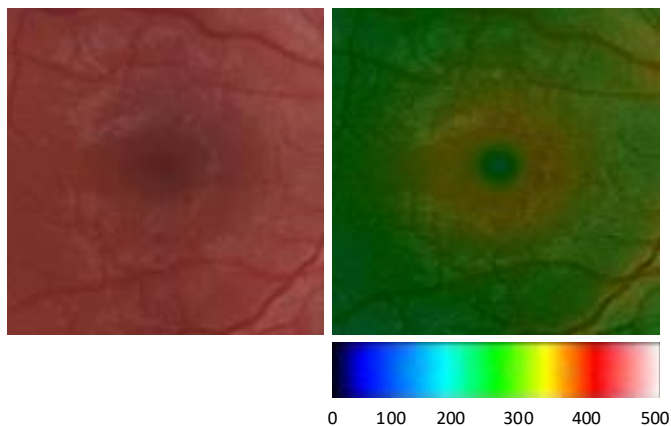


Fig. 1: The left and right image represent the correspondence between a fundus image and its thickness map image. As can be seen, each pixel's color value of the image on the right indicates a height according to color gradients below which ranges from  $0\mu\text{m}$  to  $500\mu\text{m}$ .

method is unreal and exaggerated [5] which limits its usage in real diagnosis. Furthermore, disparity map estimation, which is one of the common methods for 3D reconstruction was also applied to this problem [6], but, it totally depends on the availability of two stereo images from both eyes which is not practical. Hence, devising a method to automatically generate a heightmap image from a given fundus image is crucial.

In recent years, with the advent of Conditional Generative Adversarial Networks (cGANs) [7, 8], many researchers used this methods for image transformation tasks [7, 9, 10, 11, 12]. Recently cGANs have drawn attention in the medical field especially in the task of image-to-image translation such as

translating between CT and PET images [13, 14], denoise and correct the motion in medical images such as denoising CT images [15] and segmenting medical images [16, 17, 18]. Most of these methods benefited from the U-Net architecture [19] and its extension U-Net++ [20] which first were proposed for image segmentation.

Considering Figure 1, since our problem can be seen as an image translation task in which we want to predict a color image in which each of the pixels represents a height from  $0 \mu\text{m}$  to  $500 \mu\text{m}$  from a fundus image targeted on the macula area, cGANs can be utilized in this problem. In fact, height information is one of the crucial information that OCT devices provide to ophthalmologists and is missing in color fundus images due to their 2D nature. Hence, by extracting such information from only a fundus image, we can ease the diagnosis and management of retinal diseases with macular thickness changes.

In our cGAN setting, we used a stack of three U-Nets for generator network which we averaged on the output of them for deep supervision. Furthermore, in order to avoid problems of traditional GANs, we used Least Squares Adversarial Loss [21] instead along with perceptual loss [9] and L2-loss. For the discriminator network, we used an image-level discriminator that classifies the whole image as real or fake. To the best of our knowledge, this is the first research paper on predicting the heightmap of the macula area on fundus images using Deep Neural Networks (DNNs). We compared our approach qualitatively and quantitatively on our dataset with state-of-the-art methods in image translation and medical image translation. Furthermore, we studied the application of our method on real diagnosis cases which showed that reconstructed heightmaps can provide additional information to ophthalmologists.

## II. METHODS

### A. Network architecture

Our proposed architecture is depicted in Figure 2. As can be seen, our proposed generator architecture is consists of three stacked U-Nets. Additionally, since discriminative features in deep layers will contribute to higher performance [22], we used the output of the first two U-Net layers for deep supervision. By doing so, our network tries to learn a meaningful representation for these deep layers which will directly contribute to the final outcome. Moreover, since the amount of detail is of significance in this work, we decided to use the average operator instead of the max operator for the final output [20]. Another advantage of this architecture is that by using a stack of U-Nets, each layer can add its own level of detail to the final outcome and the details can gradually refine. Furthermore, as can be seen, we used an image-level discriminator that classifies the whole image as real or fake which using a series of Convolution-BatchNorm-LeakyReLU layers. Finally, we used  $1^{th}$ ,  $4^{th}$ ,  $6^{th}$  and  $8^{th}$  layer of the discriminator network to compute perceptual loss [10] between generated image and ground-truth image as a supervisory signal with the aim of better output.

### B. Objective functions

Our final loss function is composed of three parts which will be discussed in this section.

1) *Least-squares adversarial loss*: cGANs are generative models that learn mapping from observed image  $x$  and random noise vector  $z$  to  $\hat{y}$ , using generator  $G : x, z \rightarrow \hat{y}$ . Then the discriminator  $D$  aims to classify the concatenation of the source image  $x$  and its corresponding ground-truth image  $y$  as real  $D(x, y) = 1$ , while classifying  $x$  and the transformed image  $\hat{y}$  as fake,  $D(x, \hat{y}) = 0$ .

GANs suffer from different problems such as mode collapse or unstable training procedure despite producing plausible results in many tasks [7]. Hence, to avoid such problems we used Least Square Generative Adversarial Networks (LSGANs) [21]. The idea of LSGAN is that even samples which were classified correctly can provide signals for training. Hence, for achieving this aim, we adopted the least-squares loss function instead of the traditional cross-entropy loss used in normal cGAN to penalize data on the right side of the decision boundary but very far from it. Using this simple idea we can provide gradients even for samples that are correctly classified by the discriminator. The loss function of LSGAN for both discriminator and generator can be written as follows:

$$\begin{aligned} \min_D L_{LSGAN}(D) &= \frac{1}{2} \mathbb{E}_{x,y} \left[ (D(x, y) - b)^2 \right] + \\ &\quad \frac{1}{2} \mathbb{E}_{x,z} \left[ (D(x, G(x, z)) - a)^2 \right] \\ \min_G L_{LSGAN}(G) &= \frac{1}{2} \mathbb{E}_{x,z} \left[ (D(x, G(x, z)) - c)^2 \right] \end{aligned} \quad (1)$$

This loss functions directly operates on the logits of the output, where  $a = 0$  and  $c = b = 1$ .

2) *Pixel reconstruction loss*: Relying solely on the adversarial loss function do not produce consistent results [23]. Therefore, we also used pixel reconstruction loss here but we opted for L2-loss rather than widely used L1-loss since it performed better in reconstructing details in this specific task. The equation for L2-loss is as below:

$$L_{L2}(G) = \mathbb{E}_{x,y,z} \left[ \| y - G(x, z) \|_2^2 \right] \quad (2)$$

3) *Perceptual loss*: Despite producing plausible results using only two aforementioned loss functions, since the generated image is blurry [14] and especially in medical diagnosis small details are of significance, we used perceptual loss [24] to improve the final result. As a matter of fact, using only L2-Loss or L1-Loss results in outputs that maintain the global structure but it shows blurriness and distortions [10]. Furthermore, per-pixel losses fail to capture perceptual differences between input and ground-truth images. For instance, when we consider two identical images only shifted by some small offset from each other, per-pixel loss value may vary considerably between these two, even though they are quite similar [9]. However, by using high-level features extracted from layers of a discriminator, we can capture those discrepancies and can measure image similarity more robustly

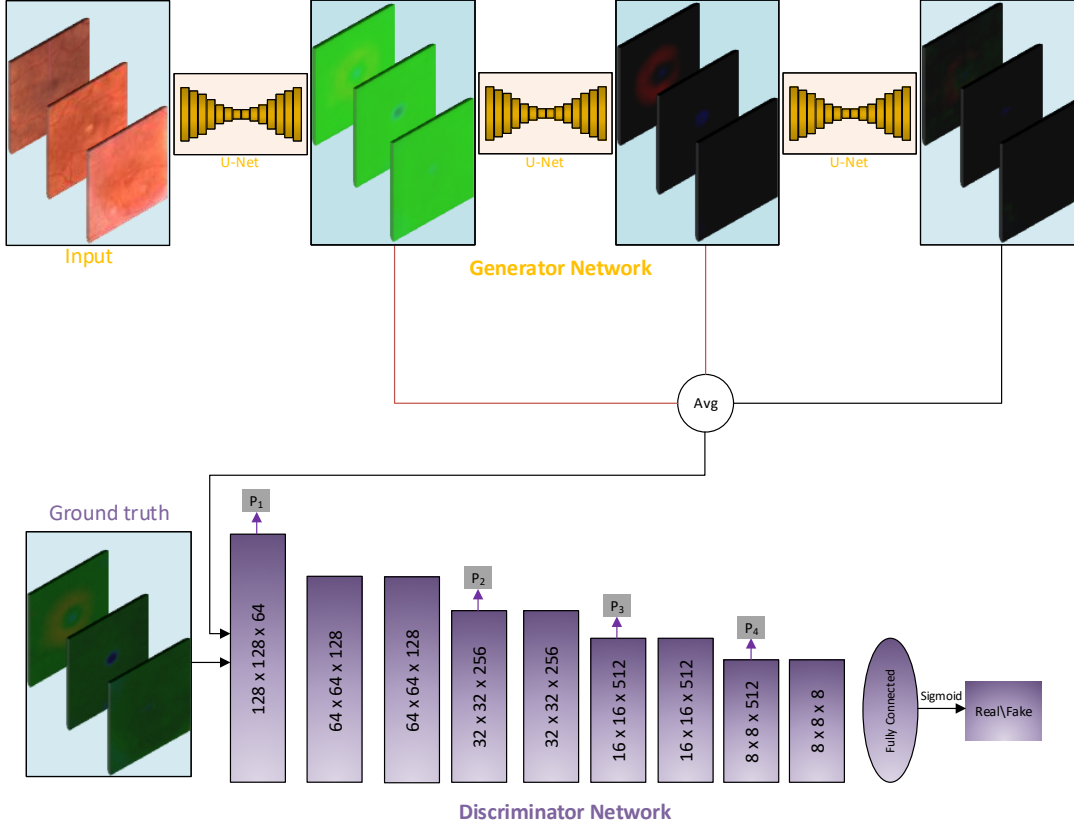


Fig. 2: The architecture of generator and discriminator in our proposed method. The red arrows indicate deep supervision.

[9]. In our work, since discriminator network also has this capability of perceiving the content of images and difference between them and pre-trained networks on other tasks may perform poorly on other unrelated tasks, we used hidden layers of discriminator network [14, 24] to extract features as illustrated in the second row of the Figure 2. The mean absolute error for  $i^{th}$  hidden layer between the generated image and the ground-truth image is then calculated as :

$$P_i(G(x, z), y) = \frac{1}{w_i h_i d_i} \| D_i(x, y) - D_i(x, G(x, z)) \|_1 \quad (3)$$

which  $w_i, h_i$  and  $d_i$  denote width, height and depth of the  $i^{th}$  hidden layer respectively and  $D_i$  means the output of  $i^{th}$  layer of the discriminator network. Finally, perceptual loss can be formulated as :

$$L_{perceptual} = \sum_{i=0}^L \lambda_i P_i(G(x, z), y) \quad (4)$$

Where  $\lambda_i$  in equation 4 tunes the contribution of  $i^{th}$  utilized hidden layer on the final loss.

Finally, our complete loss function for the generator is as below:

$$L = \alpha_1 L_{perceptual} + \alpha_2 L_{L2} + \alpha_3 L_{LSGAN} \quad (5)$$

where  $\alpha_1, \alpha_2$  and  $\alpha_3$  are the hyperparameters that balance the contribution of each of the different losses.

### III. EXPERIMENTS

#### A. Dataset and setup

The dataset was gathered from TopCon DRI OCT Triton captured at Negah Eye Hospital. Our dataset contains 3407 color fundus-heightmap pair images. Since the images in our dataset were insufficient, we used data augmentation for better generalization. However, flipping images were the only available option since by rotating images for example by  $90^\circ$ , we have vessels in a vertical position which is impossible in fundus imaging or changing brightness will change the standard brightness of a fundus image. Hence, we flipped every image in 3 different ways to generate 4 samples. Consequently, we had 13,628 images which we used 80% for training, 10% for validation and 10% for testing.

We used Tensorflow 2.0 [26] for implementing our network. We also used Adam optimizer [27] with an initial learning rate of  $1e^{-3}$  with a step decay of 0.9 per 30 steps. Moreover, we used the batch size of 8 and trained for 250 epochs to converge. Additionally, we set  $\lambda_1 = 5.0$ ,  $\lambda_2 = 1.0$ ,  $\lambda_3 = 5.0$  and  $\lambda_4 = 5.0$  in Equation 4 by trial-and-error and considering the contribution of each of them as discussed in [9, 24].

Method	SSIM	PSNR(dB)	LPIPS	MSE
pix2pix [25]	0.8596	33.9523	2.25e-03	0.0068
PAN [24]	0.8612	33.8512	2.37e-04	0.0053
MedGAN [14]	0.8659	33.2958	5.61e-05	0.0048
Proposed Method	<b>0.8823</b>	<b>34.6733</b>	<b>1.81e-05</b>	<b>0.0033</b>

TABLE I: Quantitative comparison between proposed method and other methods.

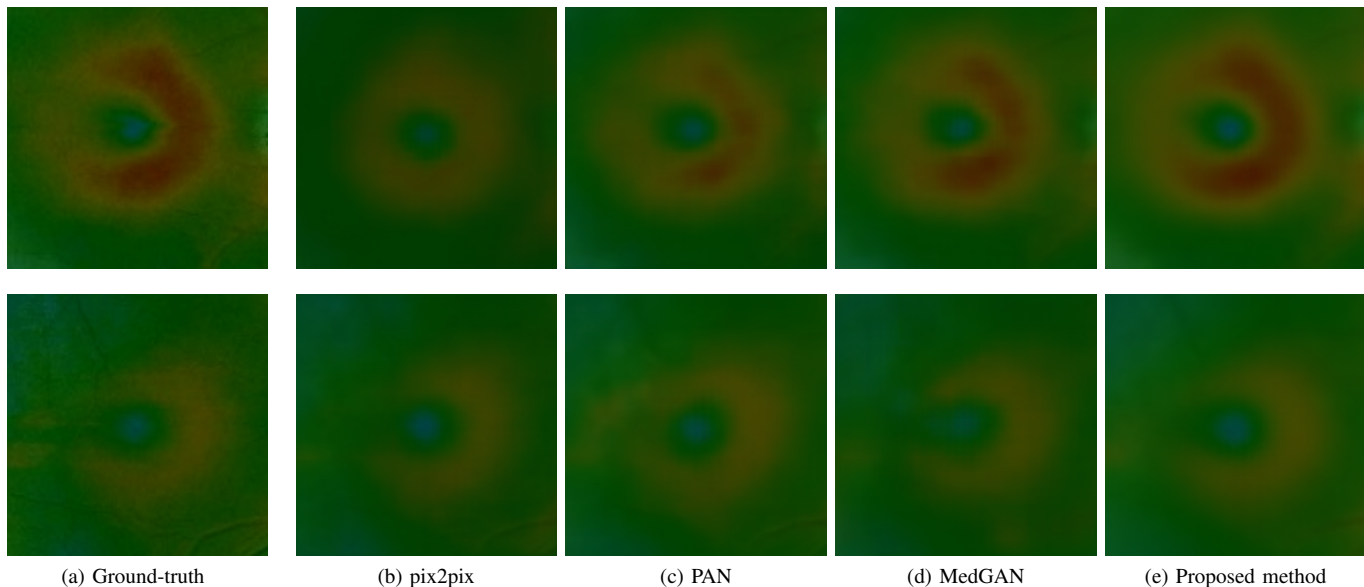


Fig. 3: Qualitative comparison between the proposed method and other methods.

### B. Evaluation metrics

we utilized a variety of different metrics to evaluate our final outcomes quantitatively such as Structural Similarity Index (SSIM) [28], Mean Squared Error (MSE) and Peak Signal to Noise Ratio (PSNR). Nevertheless, these measures are insufficient for assessing structured outputs such as images, as they assume pixel-wise independence [29]. Hence, we used Learned Perceptual Image Patch Similarity (LPIPS) [29] which can outperform other measures in terms of comparing the perceptual quality of images. For this measure, we used features extracted from the 1<sup>th</sup>, 4<sup>th</sup>, 6<sup>th</sup> and 8<sup>th</sup> layer of the discriminator network for both generate heightmap and ground-truth.

### C. Comparison with other techniques

Since this is the first method for the reconstruction of the heightmap of color fundus images using DNNs, there were no other method to directly compare our proposed method with. Hence, we compared our results with common methods which utilized cGANs such as pix2pix [25], PAN [24] and MedGAN [14]. As can be seen in Table I, Pix2pix achieved the worst results since it does not use deep supervision and it is based on L1-loss. PAN did slightly better in SSIM and MSE metrics. However, there is a huge difference between PAN and pix2pix in terms of LPIPS since PAN uses perceptual loss in the training procedure which proves the impact of using perceptual loss for training cGANs. MedGAN was designed

especially for medical image translation and, as a result, It performs better in comparison to previous general methods. However, the results are inferior to our proposed method. In fact, since we are using deep supervision in this method and carefully tuned the parameters for this particular problem, we achieve a higher value in all metrics.

Considering the qualitative comparison in Figure 3, our proposed method outperformed others in terms of reconstruction of the details. As can be seen, pix2pix missed some of the important details in first example such as bright red spots. PAN performed better at reconstructing the highly elevated parts in the first row, but it failed to reconstruct the correct shape for the second example. Finally, since MedGAN is specially designed for medical tasks, it outperformed the aforementioned methods in terms of output quality, but it was outperformed by our method and the proposed method generated the best quality images.

### D. Perceptual studies

To judge usefulness in real diagnosis cases, we conducted an experiment in which two experienced ophthalmologists were presented a series of trails each containing a reconstructed heightmap, fundus image and the ground-truth heightmap from the test set to investigate if the reconstructed heightmap and fundus image pair gives more information for the diagnosis of any retinal disease in comparison to the situation in which we have the fundus image only. For this experiment, two

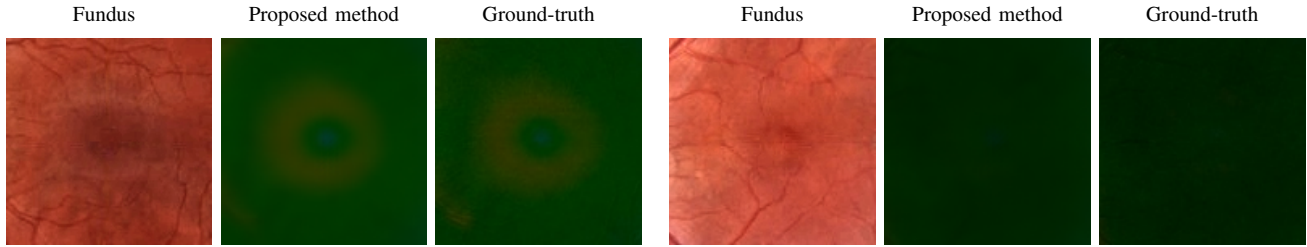


Fig. 4: Some examples from images classified as positive by two ophthalmologists.

ophthalmologists rated each image from zero to three which zero means that the reconstructed heightmap does not add more information(negative). From one to three, the heightmap is in positive class and the rating represents the level of information that it provides.

As can be seen in Table II, ophthalmologist 1 classified all images as useful for diagnosis and the mean score for all of the images is 1.94. Additionally, ophthalmologist 2 classified 92% of the outputs as positive and the mean square is 1.84. This experiment shows that although the reconstructed heightmap may seem more blurry than the ground-truth, it can still provide additional information for diagnosis especially about height information in different regions. Some positive examples are illustrated in Figure 4.

	Score		Classification
	Mean	SD	Positive %
Ophthalmologist 1	1.94	0.7669	100.00
Ophthalmologist 2	1.84	0.9553	92.00

TABLE II: Results of perceptual study.

#### IV. CONCLUSION AND DISCUSSION

In this paper, we proposed a novel framework to automatically generate heightmap images from the macula on a color fundus image. Leveraging the power of cGANs and deep supervision, this new paradigm can generate heightmaps which can provide additional information for ophthalmologists for diagnosis. Furthermore, comparisons indicate our method outperformed other methods in the task of image and medical image translation in terms of SSIM, PSNR, MSE and LPIPS metrics. However, this work is not free from limitations and further improvement is essential to improve the quality of the outputs. By investigation, we found that in most failed cases, the poor image quality caused the system to fail especially in cases in which the fundus image is blurred. This suggests that in future works, a proper pre-processing step should be employed to de-blur fundus images and improve their quality before feeding them into the network.

Finally, considering the perceptual studies which show that our reconstructed heightmap can provide additional information for the diagnosis, in future researches, we can utilize the generated heightmaps to train a classifier that is able to automatically diagnose diseases that were impossible to diagnose automatically before.

#### V. ACKNOWLEDGMENT

The authors are grateful to Dr.Ahmadih (Ophthalmologist) for grading and classifying images for our experiment.

#### REFERENCES

- [1] David Huang, Swanson EA, Lin CP, Joel Schuman, Stinson WG, Chang W, Michael Hee, Flotte T, Gregory K, Puliafito CA, and Fujimoto JG. Optical coherence tomography. *Science*, 254:1178, 01 1991.
- [2] Felipe Medeiros, Linda Zangwill, Luciana Alencar, Christopher Bowd, Pamela Sample, Remo Susanna, and Robert Weinreb. Detection of glaucoma progression with stratus oct retinal nerve fiber layer, optic nerve head, and macular thickness measurements. *Investigative ophthalmology and visual science*, 50:5741–8, 10 2009.
- [3] Ping-Sing Tsai and Mubarak Shah. Shape from shading using linear approximation. *Image Vis. Comput.*, 12:487–498, 1994.
- [4] Jini Cheriyan, B Hema, Hema Menon, and Narayanankutty K.A. 3d reconstruction of human retina from a single fundus image. 04 2012.
- [5] Peipei Wang, Fengliang Dai, Mengdie Zhao, Xiaojin Liu, and Jiulai Sun. Evaluation of retinal sfs reconstruction with oct images. pages 1–5, 10 2018.
- [6] Fan Guo, Xin Zhao, Beiji Zou, and Pingbo Ouyang. 3d reconstruction and registration for retinal image pairs. pages 364–368, 06 2018.
- [7] Ian Goodfellow, Jean Pouget-Abadie, Mehdi Mirza, Bing Xu, David Warde-Farley, Sherjil Ozair, Aaron Courville, and Y. Bengio. Generative adversarial networks. *Advances in Neural Information Processing Systems*, 3, 06 2014.
- [8] Mehdi Mirza and Simon Osindero. Conditional generative adversarial nets. 11 2014.
- [9] Justin Johnson, Alexandre Alahi, and Li Fei-Fei. Perceptual losses for real-time style transfer and super-resolution. volume 9906, pages 694–711, 10 2016.
- [10] Jia Deng, Wei Dong, Richard Socher, Li-Jia Li, Kai Li, and Fei Fei Li. Imagenet: a large-scale hierarchical image database. pages 248–255, 06 2009.
- [11] Jingming Zhao, Juan Zhang, Zhi Li, Jenq-Neng Hwang, Yongbin Gao, Zhijun Fang, Xiaoyan Jiang, and Bo Huang. Dd-cyclegan: Unpaired image dehazing via

- double-discriminator cycle-consistent generative adversarial network. *Engineering Applications of Artificial Intelligence*, 82:263 – 271, 2019.
- [12] Joshua Peter Ebenezer, Bijaylaxmi Das, and Sudipta Mukhopadhyay. Single image haze removal using conditional wasserstein generative adversarial networks. *2019 27th European Signal Processing Conference (EU-SIPCO)*, Sep 2019.
- [13] Avi Ben-Cohen, E. Klang, S. Raskin, S. Soffer, S. Ben-Haim, E. Konen, M. Amitai, and H. Greenspan. Cross-modality synthesis from ct to pet using fcn and gan networks for improved automated lesion detection. *Eng. Appl. Artif. Intell.*, 78:186–194, 2019.
- [14] Karim Armanious, Chenming Yang, Marc Fischer, Thomas Küstner, Konstantin Nikolaou, Sergios Gatidis, and Bin Yang. Medgan: Medical image translation using gans. *Computerized medical imaging and graphics : the official journal of the Computerized Medical Imaging Society*, 79:101684, 2019.
- [15] Qingsong Yang, Pingkun Yan, Yanbo Zhang, Hengyong Yu, Yongyi Shi, Xuanqin Mou, Mannudeep Kalra, Yi Zhang, Ling Sun, and Ge Wang. Low-dose ct image denoising using a generative adversarial network with wasserstein distance and perceptual loss. *IEEE Transactions on Medical Imaging*, PP, 08 2017.
- [16] Jaemin Son, Sang Jun Park, and Kyu-Hwan Jung. Retinal vessel segmentation in fundoscopic images with generative adversarial networks. 06 2017.
- [17] J. Ma, M. Wei, Z. Ma, L. Shi, and K. Zhu. Retinal vessel segmentation based on generative adversarial network and dilated convolution. In *2019 14th International Conference on Computer Science Education (ICCSE)*, pages 282–287, 2019.
- [18] Qiangguo Jin, Zhaopeng Meng, Tuan D. Pham, Qi Chen, Leyi Wei, and Ran Su. Dunet: A deformable network for retinal vessel segmentation. *Knowledge-Based Systems*, 178:149–162, Aug 2019.
- [19] Olaf Ronneberger, Philipp Fischer, and Thomas Brox. U-net: Convolutional networks for biomedical image segmentation. 05 2015.
- [20] Zongwei Zhou, Md Mahfuzur Rahman Siddiquee, Nima Tajbakhsh, and Jianming Liang. Unet++: A nested u-net architecture for medical image segmentation, 2018.
- [21] Xudong Mao, Qing Li, Haoran Xie, Raymond Y. K. Lau, Zhen Wang, and Stephen Paul Smolley. Least squares generative adversarial networks, 2017.
- [22] Chen-Yu Lee, Saining Xie, Patrick Gallagher, Zhengyou Zhang, and Zhuowen Tu. Deeply-supervised nets, 2014.
- [23] Talha Iqbal and Hazrat Ali. Generative adversarial network for medical images (mi-gan), 10 2018.
- [24] Chaoyue Wang, Chang Xu, Chaohui Wang, and Dacheng Tao. Perceptual adversarial networks for image-to-image transformation. *IEEE Transactions on Image Processing*, PP, 06 2017.
- [25] Phillip Isola, Jun-Yan Zhu, Tinghui Zhou, and Alexei Efros. Image-to-image translation with conditional adversarial networks. pages 5967–5976, 07 2017.
- [26] Martín Abadi, Ashish Agarwal, Paul Barham, Eugene Brevdo, Zhifeng Chen, Craig Citro, Greg S. Corrado, Andy Davis, Jeffrey Dean, Matthieu Devin, Sanjay Ghemawat, Ian Goodfellow, Andrew Harp, Geoffrey Irving, Michael Isard, Yangqing Jia, Rafal Jozefowicz, Lukasz Kaiser, Manjunath Kudlur, Josh Levenberg, Dan Mané, Rajat Monga, Sherry Moore, Derek Murray, Chris Olah, Mike Schuster, Jonathon Shlens, Benoit Steiner, Ilya Sutskever, Kunal Talwar, Paul Tucker, Vincent Vanhoucke, Vijay Vasudevan, Fernanda Viégas, Oriol Vinyals, Pete Warden, Martin Wattenberg, Martin Wicke, Yuan Yu, and Xiaoqiang Zheng. TensorFlow: Large-scale machine learning on heterogeneous systems, 2015. Software available from tensorflow.org.
- [27] Diederik Kingma and Jimmy Ba. Adam: A method for stochastic optimization. *International Conference on Learning Representations*, 12 2014.
- [28] Zhou Wang, Alan Bovik, Hamid Sheikh, and Eero Simoncelli. Image quality assessment: From error visibility to structural similarity. *Image Processing, IEEE Transactions on*, 13:600 – 612, 05 2004.
- [29] Richard Zhang, Phillip Isola, Alexei Efros, Eli Shechtman, and Oliver Wang. The unreasonable effectiveness of deep features as a perceptual metric. 01 2018.